

Seismicity and deformation induced by magma accumulation at three basaltic volcanoes

O. Lengline, David Marsan, Jean-Luc Got, V. Pinel, V. Ferrazzini, P. G. Okubo

▶ **To cite this version:**

O. Lengline, David Marsan, Jean-Luc Got, V. Pinel, V. Ferrazzini, et al.. Seismicity and deformation induced by magma accumulation at three basaltic volcanoes. Journal of Geophysical Research : Solid Earth, 2008, 113 (B12), pp.B12305. 10.1029/2008JB005937 . insu-00354253

HAL Id: insu-00354253
https://insu.hal.science/insu-00354253

Submitted on 26 May 2020

HAL is a multi-disciplinary open access archive for the deposit and dissemination of scientific research documents, whether they are published or not. The documents may come from teaching and research institutions in France or abroad, or from public or private research centers.

L'archive ouverte pluridisciplinaire **HAL**, est destinée au dépôt et à la diffusion de documents scientifiques de niveau recherche, publiés ou non, émanant des établissements d'enseignement et de recherche français ou étrangers, des laboratoires publics ou privés.

Seismicity and deformation induced by magma accumulation at three basaltic volcanoes

O. Lengliné,[1] D. Marsan,[1] J.-L. Got,[1] V. Pinel,[1,2] V. Ferrazzini,[3] and P. G. Okubo[4]

Received 17 July 2008; revised 18 September 2008; accepted 9 October 2008; published 18 December 2008.

[1] We analyzed the evolution of volcano-tectonic (VT) seismicity and deformation at three basaltic volcanoes (Kilauea, Mauna Loa, Piton de la Fournaise) during phases of magma accumulation. We observed that the VT earthquake activity displays an accelerating evolution at the three studied volcanoes during the time of magma accumulation. At the same times, deformation rates recorded at the summit of Kilauea and Mauna Loa volcanoes were not accelerating but rather tend to decay. To interpret these observations, we propose a physical model describing the evolution of pressure produced by the accumulation of magma into a reservoir. This variation of pressure is then used to force a simple model of damage, where damage episodes are equivalent to earthquakes. This model leads to an exponential increase of the VT activity and to an exponential decay of the deformation rate during accumulation phases. Seismicity and deformation data are well fitted by such an exponential model. The time constant, deduced from the exponential increase of the seismicity, is in agreement with the time constant predicted by the model of magma accumulation. This VT activity can thus be a direct indication of the accumulation of magma at depth, and therefore can be seen as a long-term precursory phenomenon, at least for the three studied basaltic volcanoes. Unfortunately, it does not allow the prediction of the onset of future eruptions, as no diverging point (i.e., critical time) is present in the model.

Citation: Lengliné, O., D. Marsan, J.-L. Got, V. Pinel, V. Ferrazzini, and P. G. Okubo (2008), Seismicity and deformation induced by magma accumulation at three basaltic volcanoes, *J. Geophys. Res.*, *113*, B12305, doi:10.1029/2008JB005937.

1. Introduction

[2] Active volcanoes host abundant earthquake activity. In particular, volcano-tectonic (VT) earthquakes are shear failure events and can be used as indicators of the stress state of the volcano [*McNutt*, 1996]. Here, we use VT seismicity occurring over long timescales (years) to extract information about magma accumulation in a reservoir at depth. Accumulation of magma in a reservoir produces an increase of pressure in the volcanic edifice above it. The rate of shear failures, that reflects the level of stress in the edifice, increases as this stress level grows with time. Our goal is here (1) to detect and characterize this seismic trend: which volume is affected, and the shape of the seismicity acceleration; and (2) to study how the magmatic forcing controls the rate of VT seismicity.

[3] We analyze three effusive volcanoes: Kilauea and Mauna Loa in Hawaii and Piton de la Fournaise in La Réunion. These volcanoes have all experienced recent eruptions and are well instrumented. We consider time periods when significant magma accumulation is known to have occurred at these volcanoes: From September 1977 to January 1983 at Kilauea volcano, the 1975–1984 intereruptive period at Mauna Loa volcano and the 1.2 years preceding the 1998 eruption of Piton de la Fournaise volcano.

[4] We analyzed the evolution of VT seismicity during these three periods. Previous works that focused on preeruptive seismicity rates over short timescales (a few days) reported that VT earthquake activity follows a power law acceleration [*Voight*, 1988; *Kilburn and Voight*, 1998; *De la Cruz-Reyna and Reyes-Dávila*, 2001; *Chastin and Main*, 2003; *Collombet et al.*, 2003]. Albeit the power law model appears to correctly follow the evolution of seismicity, an exponential acceleration is at least as good to reproduce the cumulative number of earthquakes during the three studied inflationary phases. Such an exponential acceleration can be explained by a model accounting for the accumulation of magma into a reservoir. This model predicts the stress history produced by the replenishment of a magma reservoir, as $\sigma(t) \sim A(1 - \exp(-Bt))$. A simple critical failure model is finally proposed to relate the stress evolution to the VT earthquake rate.

2. Magma Accumulation Periods

[5] In this section we present evidence for long periods of magma accumulation at depth for the three volcanoes, in order to select suitable time windows for analyzing the VT

[1]Laboratoire de Géophysique Interne et Tectonophysique, CNRS, Université de Savoie, Le Bourget du Lac, France.
[2]Institut de Recherche pour le Développement, IRD UR157, Marseille, France.
[3]Observatoire Volcanologique du Piton de la Fournaise, Institut de Physique du Globe de Paris, La Réunion, France.
[4]U.S. Geological Survey, Hawaiian Volcano Observatory, Hawaii National Park, Hawaii, USA.

Copyright 2008 by the American Geophysical Union.
0148-0227/08/2008JB005937$09.00

seismicity trend. During accumulation periods, magma is continuously injected into a reservoir, while the magma release from the reservoir is by comparison negligible.

[6] At Kilauea volcano, evidence for magma accumulation exists for the period preceding the January 1983 eruption. Following the 1975 Kalapana, M = 7.2 earthquake, a high rate of magma intrusion (0.18 km^3 a^{-1}) is estimated [*Cayol et al.*, 2000] on the basis of deformation measurements. Because the eruption rate during this time period is negligible (0.006 km^3 a^{-1}, *Dzurisin et al.* [1984]) compared to the intrusion rate, magma must have been stored below the volcano. The depth of the summit magma reservoir is estimated (although poorly constrained) at 3 to 5 km depth [*Tilling and Dvorak*, 1993; *Wallace and Delaney*, 1995]. Magma storage can also take place in the rift zones [*Delaney et al.*, 1990; *Cayol et al.*, 2000]. Magma rift storage is promoted, following the Kalapana earthquake, by normal faulting in the upper south flank [*Gillard et al.*, 1996]. As the Uwekahuna tiltmeter at the summit of Kilauea volcano began to show inflation following the September 1977 eruption [*Delaney et al.*, 1990], it is hypothesized that magma began accumulating under Kilauea caldera since this date [*Dzurisin et al.*, 1980]. We thus define the accumulation period at Kilauea summit between the end of the September 1977 eruption and the beginning of the 1983 eruption.

[7] The two most recent eruptions at Mauna Loa volcano took place in 1975 and 1984. Following the 1975 eruption, measurements of trilateration lines across the summit caldera showed extension [*Lockwood et al.*, 1987]. Dry-tilt measurements at the summit indicated rapid inflation just after the 1975 eruption, later becoming moderate but still continuing up to the 1984 eruption [*Lockwood et al.*, 1987]. An elastic model with a point source located at 3 km depth and with a total swelling volume of $22 \pm 6 \times 10^6$ m^3 was used to fit the deformation data recorded between 1977 and 1981. It was found to be in good agreement with observations [*Decker et al.*, 1983]. The homogeneous composition of the erupted magma during the 1984 eruption led *Rhodes* [1988] to propose that a reservoir located 3–4 km deep beneath the summit caldera has been continuously replenished in magma between the 1975 and the 1984 eruption.

[8] Significant magma accumulation is thought to have occurred at Piton de la Fournaise volcano preceding the March 1998 eruption. The 1998 eruption was the first to occur after 6 years of quiescence following the 1992 eruption. This quiescence is relatively long compared to the average 11-month intereruption interval between 1920 and 1992 [*Lahaie and Grasso*, 1998]. The estimated volume of magma release during the 1998 eruption is about 60×10^6 m^3 [*Aki and Ferrazzini*, 2000]. This volume of magma, or at least a significant part, might have been stored at depth prior to the eruption. This is suggested by the increase of the coda amplitude for summit stations after 1996 which was interpreted as resulting from the filling of reservoirs by ascending magma [*Aki and Ferrazzini*, 2000]. However, no significant deformation was detected by spaceborne radar interferometry in the 2 years preceding the 1998 eruption [*Sigmundsson et al.*, 1999]. Two microgravity field surveys (November 1997 and March 1998) encompassing the 1998 eruption revealed that a 5.4×10^{10} kg mass increase occurred during this interval [*Bonvalot et al.*, 2008]. The collected gravity data were best modeled when considering a source of mass increase at sea level. The discrepancy between the absence of surface deformation and the accumulation of magma at depth is suggested by *Bonvalot et al.* [2008] to result from magma compressibility. The beginning of the accumulation period is difficult to date. We propose that the accumulation may have started on 26 November 1996 after the occurrence of a swarm of earthquakes located at sea level beneath the central cone, the first seismic crisis since August 1992 [*Aki and Ferrazzini*, 2000]. We exclude from our analysis the last 35 h preceding the eruption, when earthquakes are caused by the dike propagation to the surface [*Battaglia et al.*, 2005]. We defined a time window corresponding to a magma accumulation induced stress extending from 26 November 1996 to 7 March 1998.

3. Data

3.1. Earthquake Catalogues

[9] We analyzed earthquake data sets corresponding to the selected time periods, as described in section 2. For Kilauea and Mauna Loa volcanoes we used the Hawaiian Volcano Observatory (HVO) earthquake catalogue. This catalogue contains all earthquakes recorded by the HVO seismic network during the 1970–2003 period. This network is specifically designed to record earthquakes related to volcanic processes. The local magnitude for each earthquake in the catalogue is reported. The average location accuracy for shallow earthquakes ($\leq$4 km) occurring near the summit is 500 m in both horizontal and vertical directions. At Piton de la Fournaise volcano we used a catalogue compiled by the Observatoire Volcanologique du Piton de la Fournaise (OVPF). The seismic moment of each earthquake in the period 1996–1999 has been estimated. We computed magnitudes on the basis moments reported in the earthquake catalogue. We use the relation $\log M_0 = 16.1 + 1.5$ m to convert moment (M_0) into magnitude (m) [*Hanks and Kanamori*, 1979]. Two different classes of earthquakes are reported: summit earthquakes and those that fall outside the summit area. Recorded earthquakes are labeled as summit events if they are located in a 2 km $\times$ 2 km area below the summit down to 6 km depth.

[10] We can draw a link between Hawaii's magnitude and Piton de la Fournaise's magnitude. We first convert magnitude into moment in Hawaii by using the relation obtained by *Zúñiga et al.* [1988]: $\log M_0 = 16.6 + 1.1\ M$, where M is the local magnitude computed in Hawaii. If we use the same relation for converting moment into moment magnitude as done for Piton de la Fournaise, we find that $1.5 \times m = 0.5 + 1.1 \times M$, where m is the magnitude reported for Piton de la Fournaise and M is the magnitude reported in Hawaii. Thus an event with a magnitude 2 at Piton de la Fournaise volcano will have a magnitude 2.3 in Hawaii. However, there is no real need in our study to have a unique magnitude scale for all volcanoes as each volcano is studied separately.

3.2. Spatial Selection of Earthquakes

[11] We selected VT earthquakes located in zones that are most likely to be influenced by the magma accumulation-induced stress. VT earthquakes generated by magma intrusions are not necessarily generated at the front of the

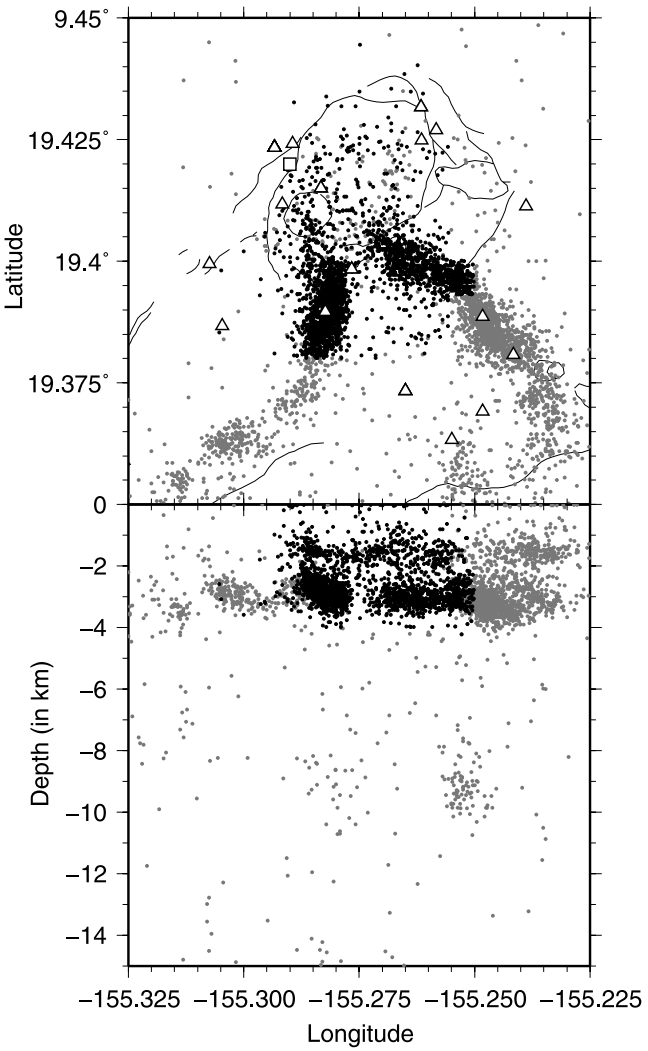


Figure 1. Map view and east-west cross section of the summit area of the Kilauea volcano. Analyzed earthquakes are represented as black dots, and rejected earthquakes are represented as gray dots. Boundaries for the earthquake selection are based on our knowledge of the stress field related to the magma reservoir, as defined by *Karpin and Thurber* [1987]. Depth range of earthquake selection extends from surface to 4 km depth. Triangles represent HVO seismic stations. The square on the rim of the caldera is the location of the Uwekahuna tiltmeter station. A large-scale map of this area is inset in Figure 2. Note that some of the black dotted earthquakes are later removed from the selection as they have a magnitude lower than the magnitude of completeness.

propagating magma body, but are mostly localized in areas of high stress concentration [*Rubin et al.*, 1998; *Rubin and Gillard*, 1998]. Local stress concentrations can be produced in volcanoes by structural heterogeneities (solidified dikes, sills). Earthquakes induced by reservoir inflation can be expected to mostly occur in these heterogeneous areas. Hence, changes in earthquake rate, in areas under the influence of the chamber inflation, directly reflect this increase in stress.

[12] At Kilauea volcano, we focused on seismicity happening in the summit area. Figure 1 shows the recorded seismicity at the summit for the analyzed time period. Seismicity is strongly clustered in the upper rift zones at about 3 km depth. We removed deep earthquakes ($z > 4$ km). These earthquakes are few during the analyzed time period and could have resulted from the stress generated by slip on a décollement plane located at 10 km depth [*Klein et al.*, 1987]. Focal mechanisms, for earthquakes occurring between 1980 and 1982 around the summit of Kilauea volcano, give clues about the local stress field. Earthquakes located within ~3 km of the caldera are expected to reflect the local stress field produced by the inflation of the summit magma reservoir [*Karpin and Thurber*, 1987]. On the contrary, dike orientations, inferred for intrusions located 1 to 2 km further downrift, are parallel to the rift zone, and

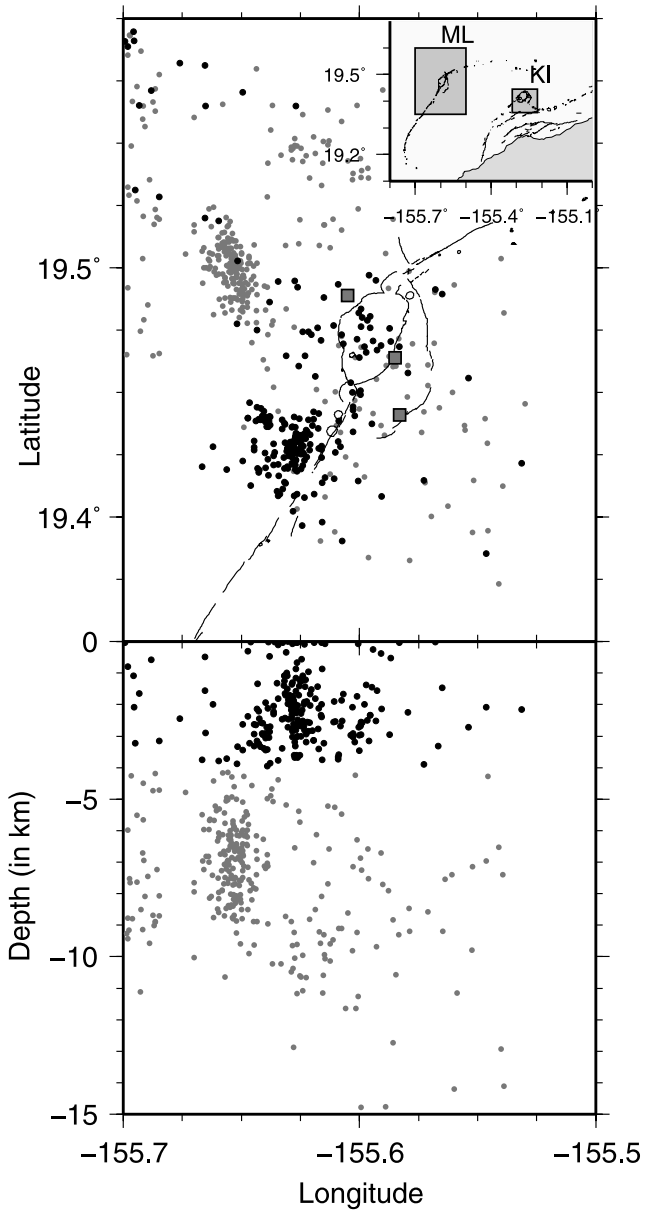


Figure 2. Same as Figure 1 but for the Mauna Loa volcano. Squares are tilt measurement locations. The inset map gives the location of the two areas around Kilauea (KI) and Mauna Loa (ML) summit displayed in this figure and in Figure 1.

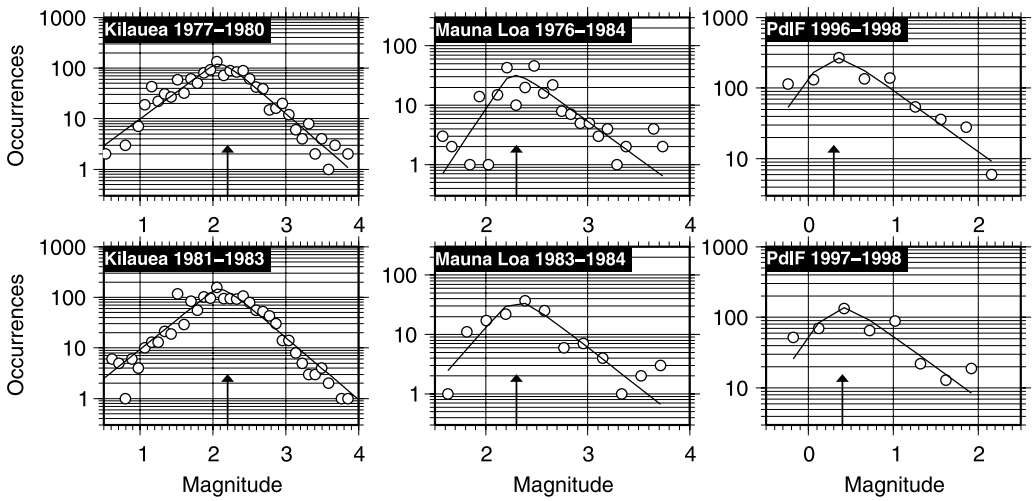


Figure 3. Number of earthquakes $n(m)$ by magnitude bins at Kilauea, Mauna Loa, and Piton de la Fournaise volcanoes. For each plot the arrow refers to the computed magnitude of completeness. The magnitude of completeness is estimated to be 2.2 and 2.3 at Kilauea and Mauna Loa volcanos, respectively, for both time periods. The magnitude of completeness is 0.3 and 0.4 at Piton de la Fournaise for the whole and the subset time period. The b value of the Gutenberg-Richter relation is 1.2 at Kilauea and Mauna Loa volcano and 0.9 at Piton de la Fournaise volcano.

are therefore not controlled by the main magma reservoir [*Karpin and Thurber*, 1987]. As a consequence we only considered earthquakes in the domain mostly influenced by the stress field originating from the chamber inflation, i.e., that are less than ~3 km of the caldera.

[13] Almost all the seismicity for the analyzed time period at Mauna Loa volcano was located in two different clusters (Figure 2). A first group of shallow earthquakes (<4 km deep) is located beneath the summit and in the upper southwest rift zone. A second group of earthquakes is found at intermediate (5–9 km) depth underneath the northwest flank. Almost all earthquakes of this deeper cluster occurred during a swarm in September 1983. A relocation study performed by *Baher et al.* [2003] on Mauna Loa earthquakes between April 1983 and April 1984 found that the relocated northwest seismicity cluster collapses onto a low dip angle fault plane at an average depth of 8 km. *Baher et al.* [2003] interpreted the structure as a failed rift zone and proposed that these earthquake's focal mechanisms are mostly controlled by the regional stress field (see also *Gillard et al.* [1992]). These earthquakes are thus related to an east-west extension that might be attributed to the edifice seaward motion on a basal plane. Given its tectonic origin, this northwest cluster is therefore not integrated in our study as its evolution is not directly linked to changes in reservoir pressure. In contrast, the shallow earthquakes are expected to occur in brittle rocks capping a magma storage reservoir [*Lockwood et al.*, 1987]. As there were no intrusions nor eruptions in the selected time period, these shallow earthquakes can be interpreted as resulting from an inflating reservoir.

[14] On Piton de la Fournaise volcano, almost all seismicity is located in a $2 \times 2 \times 3$ km^3 volume beneath the central cone, at least since 1980 when seismic monitoring started on the island and up to 1992 [*Grasso and Bachèlery*, 1995]. Earthquakes for the 1996–1998 period are also located in this same area [*Battaglia et al.*, 2005], except in the last 35 h immediately preceding the March 1998 eruption, and are thus strongly clustered in space. In the analyzed time period, more than 98% of the total seismic moment release is due to summit earthquakes. The relative absence of deep seismicity is interpreted as the result of an underdeveloped rift zone and the simplicity of the magma path [*Aki and Ferrazzini*, 2001]. Conversely, stress concentration at sea level beneath the summit area resulting from fossil dikes is thought to be responsible for the observed clustered seismicity [*Aki and Ferrazzini*, 2001]. This further suggests that the stress generated by a pressure source in the volcanic edifice will be locally high in this area, causing earthquakes to nucleate. Variations in the rate of summit earthquakes should thus correlate with stress variations in the edifice. As no eruption nor intrusion is reported in the analyzed time period, the source of stress is likely to be a pressurization of the magmatic reservoir.

3.3. Completeness

[15] We must make sure that there exists no significant changes in the magnitude of completeness during the study period, as this could lead to artificial changes in the seismicity rate. We compute the magnitude of completeness m_c on the basis the Gutenberg-Richter relation and a detection function $q(m)$ that gives the probability that an earthquake of magnitude m is effectively detected [*Marsan and Daniel*, 2007]. The number of detected earthquakes $n(m)$ with magnitude in the range $[m, m + \delta m]$, is modeled as $n(m) \sim 10^{-bm} q(m)$. We here take $q(m) = \frac{1}{2\sigma} \int_{-\infty}^{m} e^{-|m'-\mu|/\sigma} dm'$ as it empirically gives a better fit than other standard detection functions. Inversion of parameters b, μ and σ is done by a maximum likelihood search. The magnitude of completeness m_c is defined as $m_c = \mu + \sigma$ and corresponds to a 82% probability of detection. We applied this procedure to the three volcanoes.

[16] No change in the magnitude of completeness is observed at Kilauea volcano (Figure 3) between the two time periods 1977–1980 and 1981–1983. We found $m_c = 2.2$.

Table 1. Summary of the Criteria Used for Earthquake Selection at the Three Volcanoes

Volcano	Time Period	Earthquake Location	m_c
Kilauea	12/10/1977 to 03/01/1983	Shallow (<4 km deep) close to the caldera	2.2
Mauna Loa	07/07/1975 to 25/03/1984	Shallow (<4 km deep)	2.3
Piton de la Fournaise	26/11/1996 to 07/03/1998	Summit earthquakes (<6 km deep)	0.4

[17] We performed the same estimation for the selected earthquakes at Mauna Loa volcano. However, as there are fewer events (246 events for the 1976–1984 period), the variation of m_c is investigated by considering either the whole time period or the final year preceding the 1984 eruption. For the 1976–1984 time period, we find $m_c = 2.3$. We reduced the number of magnitude bins for the estimation of m_c in 1983–1984, taking $\delta m = 0.2$, to obtain $m_c = 2.3$ (Figure 3). We thus did not detect any changes in the magnitude of completeness in the catalogue for Mauna Loa earthquakes.

[18] For Piton de la Fournaise, computation of the magnitude of completeness is done for both the whole analyzed time period and for the last four months before the 1998 eruption (half of the total number of earthquakes). The estimated magnitude of completeness, m_c, is 0.4 and 0.3 for the whole and the subset analyzed time period, respectively (see Figure 3). We thus considered that the magnitude of completeness for summit earthquakes at Piton de la Fournaise is $m_c = 0.4$. We summarize our earthquake selection criteria for the three volcanoes in Table 1.

[19] We cannot ensure that earthquakes above the magnitude of completeness are representative of the whole earthquake population. However there is no way we could know whether small earthquakes (with magnitude less than the completeness magnitude) show an increasing rate or not, since not all of them are recorded, by definition. Moreover, small earthquakes, above m_c, do follow the same trends as larger ones: the opposite would imply a significant change in the b value of the Gutenberg-Richter law with time. There is no indication of such a phenomenon: on the contrary, the b value seems very stable through time for all three volcanoes (see Figure 3). Finally, a significant change in the relative rate of earthquakes smaller than m_c would translate into a significant change in the detection function q(m). Our analysis does not show this (see Figure 3). We therefore believe that the relative proportion of small earthquakes stays constant with time, and that the observed trends are representative of the trends at all magnitude bins.

4. Observations

[20] The evolution of the cumulative number of earthquakes above the magnitude of completeness for the three volcanoes is represented at Kilauea (Figure 4, left), at Mauna Loa (Figure 5, left) and at Piton de la Fournaise volcano (Figure 6). We observe a clear acceleration of the cumulative number of earthquakes with time. We also show the variation of tilt at the Uwekahuna site for the whole time period of the Kilauea data set (Figure 4, right). The station is situated on the rim of the Kilauea caldera (Figure 1). Figure 4 starts on 12 October 1977, when tremor from the September 1977 eruption ceased, and stops on 3 January 1983 at the onset of the 1983 eruption. At Mauna Loa volcano, dry-tilt data measurements were conducted during the intereruptive period 1975–1984 [*Lockwood et al.*, 1987]. These data are reported (Figure 5, right) as well as

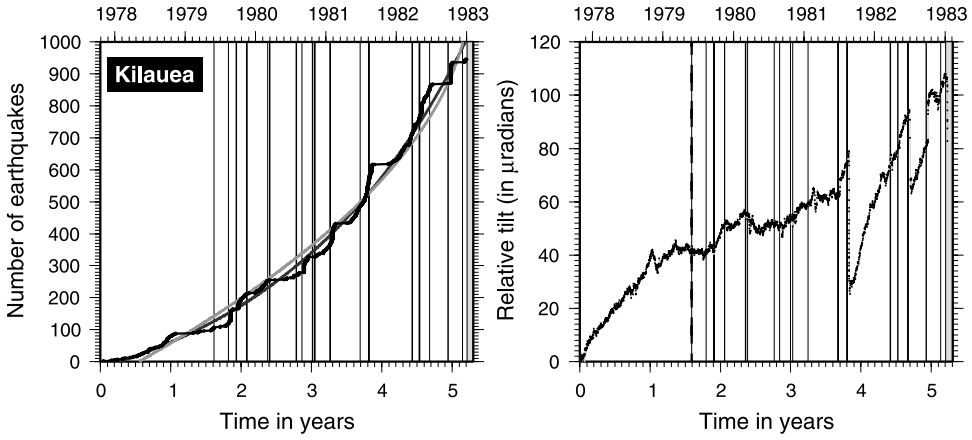


Figure 4. (left) Evolution of the cumulative number of earthquakes, $N(t)$, for the selected seismicity at Kilauea volcano between October 1977 and January 1983. Grey areas (mostly seen as black vertical lines, given the short time duration) represent known intrusion or eruption episodes. The dark grey curve represents the best exponential fit, and the light grey curve represents the best power law fit. These two curves mostly overlap. (right) Tilt measurements at the Uwekahuna site on the rim of the Kilauea caldera, at the summit of the volcano. The location of the tiltmeter site is shown in Figure 1. We display the tilt along a N60°W orientation, radial to the common center of summit inflation and deflation. Deflation and inflation events are associated with eruption/intrusion events. The increase of the tilt measurements between eruptions is associated with inflation. The dashed line indicates the time of the first intrusion that occurred after the 1977 eruption.

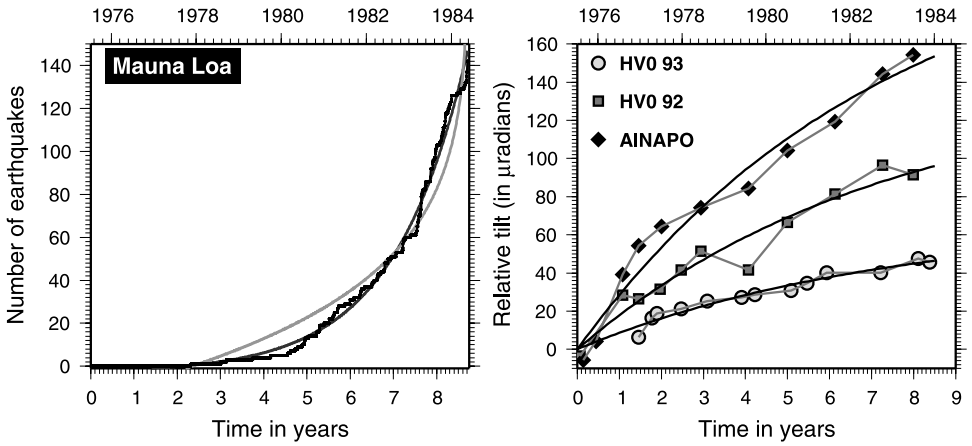


Figure 5. (left) Evolution of the cumulative number of earthquakes preceding the 1984 eruption at Mauna Loa volcano. No eruption nor intrusion took place during this time period. The best exponential fit is the dark grey curve, and the best power law fit is the light grey curve. (right) Relative tilt magnitude at Mauna Loa volcano for the intereruptive period 1975–1984. Tilts measurements were performed at three sites around the Mauna Loa caldera (Figure 2). The dark line is the best fit to the data obtained using (11).

measurement locations (Figure 2). We observe, that the acceleration of seismicity occurred while deformation rates at the same time were not increasing (they rather tend to decay). We will search for a physical model to explain the long-term variation of both the seismicity and the deformation which exhibit opposite patterns (Figure 4 and, especially, Figure 5).

[21] It should be noted that, while intrusions and eruptions occurred at Kilauea in the investigated time period, none of them stopped the acceleration of the seismicity. Indeed, the acceleration trend resumed following each of these magmatic events. This can be explained at Kilauea by the very small lava volume produced by these eruptions (the maximum lava release is occurred during the September 1982 eruption and estimated to 0.003 km^3) compared to the filling rate estimated at 0.18 km^3 a^{-1} during this time period [*Cayol et al.*, 2000]. In contrast, after the January 1983 eruption, the summit seismicity dropped drastically as only 113 earthquakes, with $m \geq 2.2$, were recorded in the selected area in the 10 years following the eruption.

5. Model

[22] A physical model explaining the observed patterns of the preeruptive seismicity rate and deformation should relate the stress history of the volcano during its preeruptive stage and the induced seismicity. It therefore needs two components:

[23] 1. A first component describes the evolution of stress, in a volcanic edifice, caused by the replenishment of a magmatic reservoir. This model assumes a magmatic

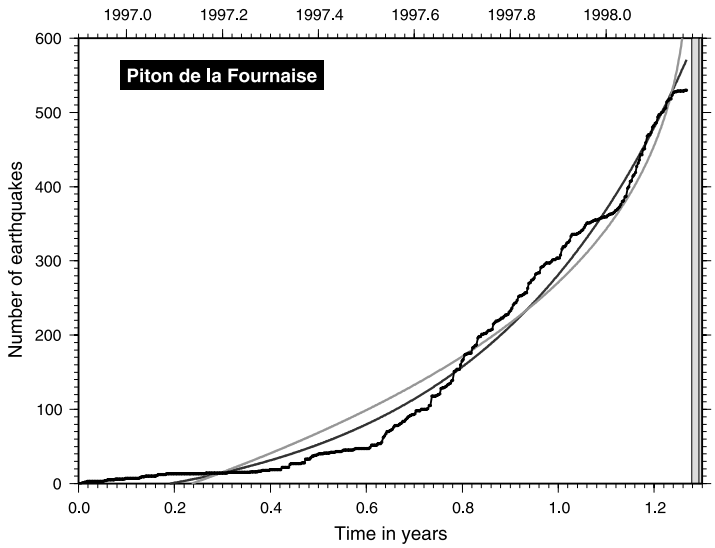


Figure 6. Evolution of the cumulative number of earthquakes in the ~1.2 years preceding the 1998 eruption at Piton de la Fournaise. No eruption nor intrusion took place during this time period. The best exponential fit is the dark grey curve, and the best power law fit is the light grey curve. These two curves overlap.

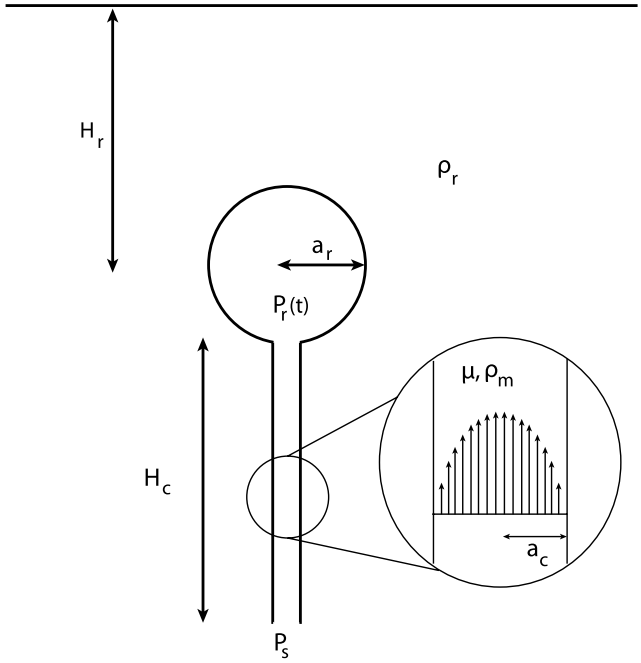


Figure 7. Sketch showing the geometry of the model. A spherical reservoir at depth H_r and of radius a_r is fed by magma flowing through a cylindrical conduit of radius a_c and length H_c. The magma is defined by its viscosity μ and its density ρ_m. The density of rocks surrounding the magma chamber is ρ_r. P_s is the source pressure and is supposed to be constant. $P_r(t)$ is the reservoir pressure, which varies with time.

chamber surrounded by a purely elastic medium and a constant magma source overpressure.

[24] 2. A second component is a seismicity model which links the stress history to a VT earthquake rate. Our approach is equivalent to a damage model in a heterogeneous medium, and is based on a critical point hypothesis.

[25] Our aim is to model the observed variations with a minimum number of parameters. Many volcanic phenomena, possibly leading to earthquake nucleation, are disregarded in this study. These include gas pressure increase produced by magma cooling, heating of groundwater, tectonic or dynamic strain. However, the magma accumulation process is the only common phenomenon identified at the three studied volcanoes for the whole analyzed time periods. We therefore consider it as being the only source of stress variation in the edifice.

5.1. A Model of Magma-Induced Stress

[26] Our model is based on the inflation of a spherical magma reservoir at depth H_r and of radius a_r fed by a conduit of length H_c and radius a_c (Figure 7). The ascent of magma in a cylindrical conduit, in laminar flow conditions is described by the Poiseuille law, which gives the mass flux Q at height z as

$$Q = \frac{\pi a_c^4}{8\mu}\left[-\frac{dP}{dz} - \rho_m g\right] \tag{1}$$

where dP/dz is the vertical pressure gradient, μ is the magma viscosity and ρ_m the magma density. We assume the magma viscosity and density to be constant over all the conduit. The different pressure sources acting on the magma in the pipe are the following:

[27] 1. The source pressure P_s corresponds to the pressure at the bottom of the pipe, which is considered as constant. This pressure is the sum of the lithostatic pressure P_{litho} at the source depth z_s and an overpressure ΔP_s:

$$P_s = P_{litho}(z_s) + \Delta P_s \tag{2}$$

[28] 2. The reservoir pressure $P_r(t)$ corresponds to the pressure at the top of the pipe which increases as the reservoir is fed from the source. It is the sum of the lithostatic pressure at the reservoir depth z_r and an overpressure $\Delta P_r(t)$:

$$P_r(t) = P_{litho}(z_r) + \Delta P_r(t) \tag{3}$$

In the following we will consider that

$$\Delta P_r(t) = \Delta P_r^0 + \Delta P(t) \tag{4}$$

where ΔP_r^0 is the initial overpressure at the beginning of the accumulation and $\Delta P(t = 0) = 0$.

[29] Accounting for these different sources of pressure and setting ρ_r as the density of rocks surrounding the magma chamber, it follows that

$$Q(t) = \frac{\pi a_c^4}{8\mu H_c}[\Delta P_s - \Delta P_r(t) + (\rho_r - \rho_m)gH_c] \tag{5}$$

[*Pinel and Jaupart*, 2003]. We link the volume of injected magma $\Delta V_{in}(t)$ into the reservoir with its overpressure variation $\Delta P(t)$ through the expression [*Delaney and McTigue*, 1994]

$$\Delta V_{in}(t) = \Delta P(t)\frac{\pi a_r^3}{G} \tag{6}$$

where G is the rigidity modulus. We further assume that no magma leaves the chamber during the accumulation period. This assumption is valid for all three volcanoes, and even for Kilauea volcano where the erupted volume is insignificant compared to the filled volume during the analyzed period. It then follows from (5) and (6) that

$$\frac{d\Delta P(t)}{dt} = \frac{Ga_c^4}{8\mu H_c a_r^3}(P - \Delta P(t)) \tag{7}$$

where P is a constant term with $P = \Delta P_s - \Delta P_r^0 + (\rho_r - \rho_m)gH_c$. This is a simple differential equation, which solution is given by

$$\Delta P(t) = P\left(1 - \exp\left(\frac{-t}{\tau}\right)\right) \tag{8}$$

where

$$\tau = \frac{8\mu H_c a_r^3}{Ga_c^4} \tag{9}$$

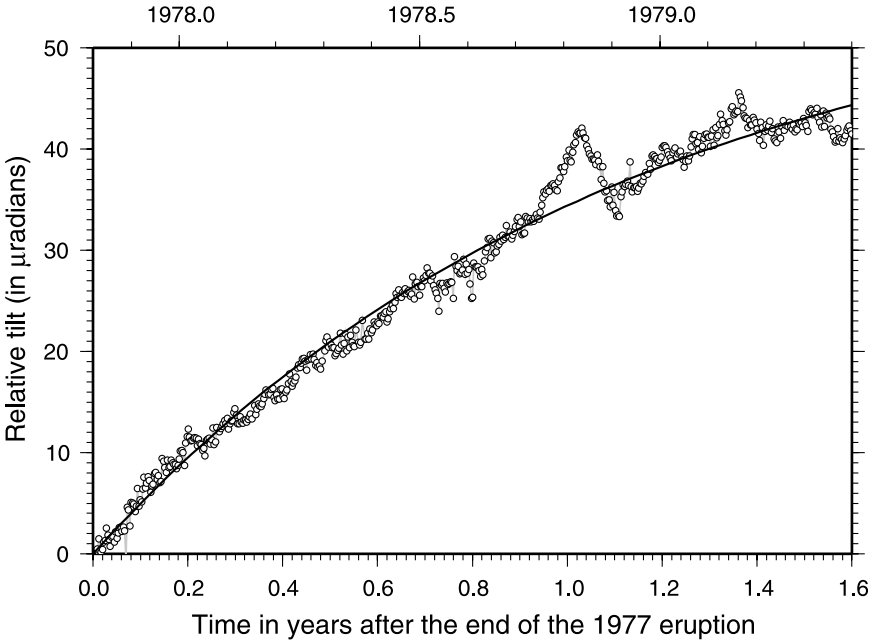


Figure 8. Relative tilt magnitude between 12 October 1977 (end of the 1977 eruption) to the first intrusion after this eruption, on 29 May 1979 (dotted vertical line on Figure 4). The dark line is the best fit to the data obtained using (11).

is a characteristic time. As the magmatic stress-induced seismicity is strongly clustered in space at the three volcanoes for the analyzed time periods and did not show any migration, it is reasonable to consider that the variation of pressure at the seismicity location will be proportional to (8). As $\Delta P(t)$ can be expressed as a function of the maximum vertical uplift $u_z^{\max}(t)$ (i.e., the vertical uplift at the inflation center) with

$$\Delta P(t) = \frac{GH_r^2}{a_r^3(1-\nu)} u_z^{\max}(t) \tag{10}$$

where v is the Poisson's ratio, one can obtain the evolution of $u_z^{\max}(t)$ from (8) and (10):

$$u_z^{\max}(t) = \frac{(1-\nu)a_r^3}{GH_r^2} P\left(1 - \exp\left(\frac{-t}{\tau}\right)\right) \tag{11}$$

[30] This gives the evolution of the vertical uplift at the top of the magmatic reservoir, i.e., where it is maximum. The evolution of $u_z(t)$ at different locations around the reservoir is recovered by

$$u_z(t,r) = u_z^{\max}(t)\left[1 + (r/H_r)^2\right]^{-3/2} \tag{12}$$

where r is the horizontal distance between the observation point and the inflation center. The uplift $u_z(t, r)$ will thus evolve with the same characteristic time τ as $u_z^{\max}(t)$, in a purely elastic medium.

[31] Our model does not account for magma compressibility. As proposed by *Johnson* [1992], magma compressibility may accommodate the volume of newly added magma. We hypothesize that the variation of pressure during the magma accumulation phase is small, compared to the total pressure in the reservoir. This is likely to be the case as the lithostatic stress at reservoir depths for the three studied volcanoes is of the order of 100 MPa. Conversely, the order of magnitude of overpressure detected before eruptions at Piton de la Fournaise volcanoes is close to 1 MPa [*Brenguier et al.*, 2008]. By applying the results of *Johnson* [1992] and *Johnson et al.* [2000] we find that the effect of compressibility is to change the timescale of τ but the evolution of stress will remain similar to (8). Thus, at Piton de la Fournaise volcano, where compressibility is thought to have played a role in the pre-1998 eruption, the stress history will remain similar to the other volcanoes.

[32] The variation in tilt at Kilauea volcano is fitted with an exponential model following the form of (11). The fit is not performed over the whole time period, as this would include deflation events that occurred late in this time period. We only considered measurements that reflect the inflation of the edifice, and that are not affected by deflation or inflation caused by a localized batch of magma. Indeed, local deformations, close to the tiltmeter site, can produce strong amplitude signals but are not necessarily related to a strong change of pressure in the reservoir. We thus only take into account measurements taken before the first intrusion that occurred after the 1977 eruption (i.e., the 29 May 1979 intrusion event [*Klein et al.*, 1987]).

[33] The evolution of the tilt data is well described by (11), see Figure 8. The time constant τ is equal to 1.13 years $\pm$0.05 year at the 95% confidence level, and R^2 = 0.98. Although the time resolution of tilt data at Mauna Loa volcano is not as good as for Kilauea volcano, a slowing down of the tilt increase is observed during the intereruptive period (Figure 5, right). Relative tilt time series are modeled with (11) but we impose the time constant τ to be the same at the three tiltmeter sites. The least squares estimates is τ =

7.3 years with a [5.1–12.8] years 95% confidence interval. This time constant is not well constrained as there are only a few data points at early times.

[34] Evidence for the $a(1 - \exp(bt))$ growth of the vertical displacement due to the filling of a magmatic reservoir can also be found in examples of the cycles of inflation-deflation episodes after the beginning of the 1983 eruption in the middle east rift zone, in 1983. *Dvorak and Okamura* [1987] found that vertical displacements at the surface during inflationary stages match an evolution similar to (11). One can also consider the case of the Grimsvötn volcano, Iceland: Following the 1998 eruption, vertical displacement appears to follow the same exponential trend [*Sturkell et al.*, 2003]. Another example of an exponentially decaying vertical displacement rate is also suggested for Westdahl volcano, Alaska [*Lu et al.*, 2003]. The inflation at Westdahl volcano was modeled by an exponential function with a time constant of about 6 years [*Lu et al.*, 2003]. A last example is provided from recorded vertical displacements at Kilauea volcano during a volcanic crisis in 1996. Cycles of inflation of the order of 10 μm recorded on a timescale of 1 to 3 min were followed by rapid deflations [*Ohminato et al.*, 1998]. The evolution of the vertical displacement during inflationary stages is thought to result from magma accumulation into a subhorizontal crack and displays an evolution similar to (11) [*Ohminato et al.*, 1998]. As the vertical displacement observed during inflationary stages obeys (11), at least to the first order, it is reasonable to suppose that the change in pressure in the rock surrounding the magmatic reservoir will follow (8).

5.2. Relating Stress and VT Earthquakes

[35] The analyzed seismicity at Kilauea and Mauna Loa occurs primarily along the upper rift zones. These areas are very heterogeneous as solidified dikes, veins and joints are present. At Piton de la Fournaise, the summit area of the volcano is envisioned as a network of dikes and sills [*Lénat and Bachèlery*, 1990]. These heterogeneities create stress concentrations, thought to be responsible for the observed clustering of earthquakes. *Hill* [1977] proposed that stress concentrations are produced in the intervals between adjacent dikes. In *Hill*'s [1977] model, VT earthquakes occur on oblique faults linking two dikes. We here postulate that stress concentrations, in the damaged areas, induce shear failure earthquakes wherever the shear stress is greater that the normal stress.

[36] The complex summit structure of Piton de la Fournaise and power law distributions characterizing many phenomena related to this volcano, has led *Grasso and Bachèlery* [1995] to conclude that the dynamics of the volcano is governed by self-organized criticality. The complexity of this dynamics is well recovered by a cellular automaton model characterized by a critical pressure [*Lahaie and Grasso*, 1998]. We interpret summit and near summit seismicity at the three studied volcanoes as the result of brittle failure in a disordered medium. The global breakdown of the system is represented by a first-order transition of the shallow part of the edifice and is symbolized by an eruption. Studies of critical ruptures in heterogeneous media reveal that the evolution of cumulative damage D, prior to the global failure, with the controlling stress σ, exhibits a relation of the form [*Garcimartin et al.*, 1997; *Zapperi et al.*, 1997; *Johansen and Sornette*, 2000]

$$D = A + B(\sigma_c - \sigma)^{-\gamma} \tag{13}$$

where σ_c is the critical stress and $\gamma \in [0;1]$, is the critical exponent. We simply interpret the cumulative damage, D, as the cumulative number of earthquakes. A uniformly increasing stress $d\sigma/dt$ = const produces a power law acceleration near the critical point as stated by (13). The acceleration takes a different form if the forcing stress follows the evolution of pressure as found in (8):

$$D(t) = A + B\left[\sigma_c - P_0 - P\left(1 - \exp\left(\frac{-t}{\tau}\right)\right)\right]^{-\gamma} \tag{14}$$

where $P_0 = P_{litho}(z_r) + \Delta P_r^0$ is the initial stress of the system. An eruption will occur if the shallow part of the volcanic edifice ruptures, i.e., when the critical stress is reached. Thus, an eruption happens if $P + P_0 > \sigma_c$. If the asymptotic final stress of the system, $P + P_0$, is assimilated to the critical stress σ_c, (14) then becomes

$$D(t) = A + B' \exp\left(\frac{\gamma t}{\tau}\right) \tag{15}$$

i.e., we obtain an exponential acceleration of the seismicity. If $P + P_0 > \sigma_c$, a deviation from the pure exponential form will appear. In this case the full form of the stress evolution (14) should be used to quantify the evolution of seismicity. However, this deviation from the exponential form will remain low if $(\sigma_c - P_0 - P)/P$ or t/τ is low.

6. Discussion

[37] We presented a coherent model to link the stress history with deformation and seismicity for a basaltic volcano undergoing a magma replenishment phase. We now compare how accurately this model is able to recover the observed seismicity and deformation trends.

[38] For each earthquake time series (Figures 4–6), an exponential and a power law fit are performed. The fits are done by minimizing a least squares criterion. The power law fit is performed as a reference fit. It is generally reported as a good phenomenological model for earthquake rates in preeruptive phases [*Voight*, 1988; *Kilburn and Voight*, 1998; *Chastin and Main*, 2003; *Collombet et al.*, 2003]. Denoting $N(t)$ the cumulative number of earthquakes at a time t following the beginning of magma accumulation, the two fits are performed using three parameters a, b and c: $N(t) = a \times \exp(b \times t) + c$ and $N(t) = a \times (t_e - t)^b + c$, where t_e is the time of eruption, with all time in years.

[39] Both the power law and the exponential model appear to match remarkably well the evolution of the seismicity for all three volcanoes. The goodness of fits are evaluated with the coefficient of determination, R^2, which is derived from the maximum likelihood and can be written, $R^2 = 1 - \Sigma_i (y_i - f_i)^2/\Sigma_i (y_i - \bar{y})^2$, where $\mathbf{y}$ is the observed data vector and $\mathbf{f}$ is the modeled data vector, the overbar denotes the mean. The R^2 coefficient is never lower than 99% for the exponential model. Comparatively, we obtain

Table 2. Parameters Deduced From Fits of an Exponential and a Power Law Model on Seismicity Data[a]

	Exponential Model				Power Law Model			
Volcano	a	b (a^{-1})	c	R^2	a	b (a^{-1})	c	R^2
Kilauea	210	0.345	−232	0.99	−529	0.508	1160	0.98
Mauna Loa	0.872	0.591	−3.00	0.99	−250	0.135	322	0.93
PdlF	31.5	2.35	−49.3	0.99	−881	0.273	892	0.96

[a]Pdlf refer to the Piton de la Fournaise volcano.

R^2 = 0.98, 0.93 and 0.96 for the power law fits at Kilauea, Mauna Loa and Piton de la Fournaise, respectively. The exponential fits still remain good when setting $c = 0$ ($R^2 >$ 98%). Table 2 details all the parameter values obtained. Moreover a good exponential fit and power law fit are recovered when increasing m_c for the three volcanoes or when the total moment released is fitted rather than the number of earthquakes. In these two cases, time constants obtained when fitting with the exponential model are similar to those reported in Table 2. The exponential form of the evolution of the seismicity is thus consistent with the prediction of our proposed model (equations (14) and (15)).

[40] Furthermore we can investigate if the characteristic time proposed in our model is coherent with the one obtained when fitting the data. At Kilauea volcano for example, we find τ = 1.13 years when fitting the tilt data. The order of magnitude of this value of τ can be obtained using typical estimates of the parameters entering its definition (equation (9)), e.g., using μ = 100 Pa s, G = 7.5 GPa, a_r = 2 km, H_c = 20 km and a_c = 0.5 m. There are, however, considerable uncertainties on most parameters, strongly affecting the value of τ. For example, slight changes in the poorly constrained conduit radius, a_c, will cause important variations of τ. Finally, it is interesting to compare the time constant deduced from the seismicity and the one obtained by fitting the tilt data. We hypothesize that the evolution of the seismicity at Kilauea volcano can be described by (15). As γ = 1/2 in the mean-field theory [*Zapperi et al.*, 1997], we should have $\tau_{seis} = 2\ \tau_{tilt}$. At Kilauea volcano, we obtained 2.90 years for τ_{seis} and 2.27 years for $2\tau_{tilt}$, and hence two values that are coherent with our model. The same relation should also be verified at Mauna Loa volcano if we considered (15) as a valid description of the underlying phenomenon. We obtained τ_{seis} = 1.7 years and $2\tau_{tilt}$ = 14.6 years at Mauna Loa volcano. This discrepancy between the two time constants can be explained if the asymptotic final stress at Mauna Loa volcano is larger than the critical stress, thus one should use (14) as the correct model. We test this hypothesis by fitting a model similar to (14) to the Mauna Loa seismicity. This model can be written $N(t) = a + b(c + \exp(t/(2\tau_{tilt})))^{-0.5}$ where τ_{tilt}, the time constant deduced from the geodetic data is forced in the model. The resulting fit has a R^2 = 97% lower than the exponential form of (15) but still better than the power law fit and can be hypothesized as a reasonable scenario for Mauna Loa.

[41] Power law accelerations of the rate of summit VT seismicity have been found preceding dike intrusions or eruptions at Kilauea and Piton de la Fournaise [see *Chastin and Main*, 2003; *Collombet et al.*, 2003]. However, these accelerations are obtained only after stacking over multiple sequences and are no more than 10 days long. Eruptions at Piton de la Fournaise are preceded by short (∼10 days) pressurization of the edifice [*Brenguier et al.*, 2008]. A power law acceleration of the seismicity has also been found at andesitic volcanoes for a single eruption at the same ∼10 days timescale, i.e., at Bezymianny, Kamchatka [*Voight*, 1988] and Soufriere Hills, Montserrat [*Kilburn and Voight*, 1998]. The difference between a power law model and an exponential model has implication on the physical mechanism driving the deformation. Because both models are linked to the stress evolution, the difference between the two models reflects a difference in the loading process. The exponential model which is proposed is related to slow, decelerating condition. This is the case of the magma accumulation. The power law model is generally related to a constant stressing rate model [e.g., *Johansen and Sornette*, 2000]. This might happen when the evolution of pressure is fast, as during the propagation stage of a single dike. It thus provides an explanation about the limited timescale of power laws observations. Furthermore, the power law signature of an intruding dike can be hidden by the global process materialized by the magma accumulation. This might be a reason why the power law associated with eruptions is only recovered on average at basaltic volcanoes. It is also remarkable to note that (14) can also leads to a power law acceleration. This case might happen on a limited timescale during the late stage of failure ($t \gg \tau$) if $P + P_0 > \sigma_c$. Albeit the evolution of seismicity remains exponential during most of the accumulation phase, at the last stage of failure, the evolution will take a different form with $D(t) \propto (t_c - t)^{-\gamma}$, where t_c is a critical time defined by $t_c = -\tau \ln((P + P_0 - \sigma_c)/P)$.

[42] In the case of a basaltic volcano, the propagation of a single dike may not release the total pressure stored in the edifice and will possibly only connect a small magma pocket with limited storage capacity to the surface. This event will thus not affect the increase of pressure associated with the replenishment of the magma reservoir unless the whole edifice is so close to failure that all pockets are interconnected and the entire edifice erupts [*Lahaie and Grasso*, 1998]. The critical stress of the volcanic edifice is thus not necessarily associated with all eruptions. The small eruptions are part of the global process leading to a major eruption which stopped the loading process, and released a largest volume of magma. This major eruption materialized the edifice failure. This might explain why an acceleration of the seismicity is observed during the whole time interval, 1977–1983, at Kilauea volcano despite the occurrence of multiple eruptions. At andesitic volcanoes, eruptions lead to an almost complete relaxation of the pressure. This is suggested by the longer time interval between eruptions with higher explosivity index [*Simkin and Siebert*, 2000].

[43] One notable feature of power law accelerations is that they could provide an a priori prediction of the eruption onset time [*Kilburn and Voight*, 1998]: The VT activity, $N(t) = a \times (t_e - t)^b + c$, becomes singular at t_e. However, a power law acceleration is only found when averaging over multiple sequences at basaltic volcanoes [*Chastin and Main*, 2003; *Collombet et al.*, 2003], and the short timescale of the acceleration at andesitic volcanoes limits its applicability for mitigating volcanic hazards [*Kilburn and Sammonds*, 2005].

[44] At last, we would like to emphasize that the physical model we proposed could not have been resolved on the basis seismicity data alone. Such an analysis, limited to seismicity data, would not have been able to reject a power law model. It is the conjunction of both deformation and seismicity data that allows us to discriminate between possible models. It highlights the importance of building models based on the evolution of multiple parameters.

7. Conclusion

[45] We showed here that during the three studied phases of magma accumulation, VT seismicity, close to inflation centers, can be well described by an exponential increase. This increase of seismicity occurred while deformation rates recorded at the same time at Kilauea and Mauna Loa volcano were decreasing. We proposed a model that accounts for both seismicity and deformation. We studied the evolution of pressure of a magmatic reservoir undergoing a replenishment from a source region at depth. A constant source overpressure was hypothesized and the evolution of the reservoir pressure is controlled by the addition of new magma. However, the increase of pressure in a reservoir, reduces the rate of newly entering magma in the reservoir, and thus introduces slow, decelerating, loading condition. These mechanisms led to a pressure rate exponentially decaying over the time of magma accumulation process. The same evolution was obtained for vertical deformation if an elastic medium is assumed. This shape of deformation is often observed on volcanoes during inflation stages and appears to explain the deformation at Kilauea and Mauna Loa. Finally, a simple model of rupture was used to link the load history to the evolution of seismicity. This simple model is able to reproduce the observed exponential evolution of the seismicity. We thus propose that magma accumulation at basaltic volcanoes may be characterized by a broad scale process and that this process can be identified by a combined analysis of both geodetic and seismic data.

[46] We finally propose that a precursory pattern emerges at long time scales (years) and is likely to be related to the accumulation of magma in a reservoir, at least for the three studied volcanoes. This precursory phenomenon might be represented by an exponential acceleration of the seismicity. Vertical displacement at the surface can also attest for the accumulation of magma. However, displacements are difficult to detect if the reservoir is deep. The deformation pattern may also be highly sensitive to local, small shallow intrusions or eruptions. The evolution of the seismicity during inflationary stages may thus provide indirect information about the state of stress in the edifice. Unfortunately, it will not allow for a prediction about the timing of future eruptions, as no singularity is present in the model. However, the knowledge of an ongoing magmatic reservoir replenishment might be helpful for mitigating volcanic hazards as it provides the timeliness for risk management and further instrumentation deployment on and around the volcano.

[47] **Acknowledgments.** We thank Jean-Robert Grasso for numerous discussions and Servando De la Cruz-Reyna for useful comments. We also thank two anonymous reviewers and the Associate Editor for their thoughtful reviews. We thank Asta Miklius for providing us tilt data at Kilauea. We thank the staff of the Hawaiian Volcano Observatory and of the Observatoire Volcanologique du Piton de la Fournaise for their continuous effort to maintain operational their seismic networks. Most of the figures were produced using the GMT Software [*Wessel and Smith*, 1991]. O.L. is supported by European Commission FP6 project VOLUME (contract 18471).

References

Aki, K., and V. Ferrazzini (2000), Seismic monitoring and modeling of an active volcano for prediction, *J. Geophys. Res.*, *105*, 16,617–16,640.

Aki, K., and V. Ferrazzini (2001), Comparison of Mount Etna, Kilauea, and Piton de la Fournaise by a quantitative modeling of their eruption histories, *J. Geophys. Res.*, *106*, 4091–4102.

Baher, S., C. Thurber, K. Roberts, and C. Rowe (2003), Relocation of seismicity preceding the 1984 eruption of Mauna Loa Volcano, Hawaii: Delineation of a possible failed rift, *J. Volcanol. Geotherm. Res.*, *128*, 327–339.

Battaglia, J., V. Ferrazzini, T. Staudacher, K. Aki, and J.-L. Cheminée (2005), Pre-eruptive migration of earthquakes at the Piton de la Fournaise volcano, Réunion Island, *Geophys. J. Int.*, *161*, 549–558.

Bonvalot, S., D. Remy, C. Deplus, M. Diament, and G. Gabalda (2008), Insights on the March 1998 eruption at Piton de la Fournaise volcano (La Réunion) from microgravity monitoring, *J. Geophys. Res.*, *113*, B05407, doi:10.1029/2007JB005084.

Brenguier, F., N. M. Shapiro, M. Campillo, V. Ferrazzini, Z. Duputel, O. Coutant, and A. Nercessian (2008), Towards forecasting volcanic eruptions using seismic noise, *Nat. Geosci.*, *2*, 126–130.

Cayol, V., J. H. Dieterich, A. T. Okamura, and A. Miklius (2000), High magma storage rates before the 1983 eruption of Kilauea, Hawaii, *Science*, *288*, 2343–2345.

Chastin, S. F. M., and I. G. Main (2003), Statistical analysis of daily event rate as precursor to volcanic eruptions, *Geophys. Res. Lett.*, *30*(13), 1671, doi:10.1029/2003GL016900.

Collombet, M., J.-R. Grasso, and V. Ferrazzini (2003), Seismicity rate before eruptions on Piton de la Fournaise volcano: Implications for eruption dynamics, *Geophys. Res. Lett.*, *30*(21), 2099, doi:10.1029/2003GL017494.

Decker, R. W., R. Y. Koyanagi, J. J. Dvorak, J. P. Lockwood, A. T. Okamura, K. M. Yamashita, and W. R. Tanigawa (1983), Seismicity and surface deformation of Mauna-Loa volcano, Hawaii, *Eos Trans. AGU*, *64*(37), 545.

De la Cruz-Reyna, S., and G. Reyes-Dávila (2001), A model to describe precursory material-failure phenomena: Applications to short-term forecasting at Colima volcano, Mexico, *Bull. Volcanol.*, *63*, 297–308, doi:10.1007/s004450100152.

Delaney, P. T., and D. F. McTigue (1994), Volume of magma accumulation or withdrawal estimated from surface uplift or subsidence, with application to the 1960 collpase of Kilauea volcano, *Bull. Volcanol.*, *56*, 417–424.

Delaney, P. T., R. S. Fiske, A. Miklius, A. T. Okamura, and M. K. Sako (1990), Deep magma body beneath the summit and rift zones of Kilauea volcano, Hawaii, *Science*, *247*, 1311–1316.

Dvorak, J. J., and A. T. Okamura (1987), A hydraulic model to explain variations in summit tilt rate at Kilauea and Mauna-Loa volcanoes, in *Volcanism in Hawaii*, *U. S. Geol. Surv. Prof. Pap.*, *1350*, 1281–1296.

Dzurisin, D., L. A. Anderson, G. P. Eaton, R. Y. Koyanagi, P. W. Lipman, J. P. Lockwood, R. T. Okamura, G. S. Puniwai, M. K. Sako, and K. M. Yamashita (1980), Geophysical observations of Kilauea volcano, Hawaii. 2. Constraints on the magma supply during November 1975–September 1977, *J. Volcanol. Geotherm. Res.*, *7*, 241–269.

Dzurisin, D., R. Y. Koyanagi, and T. T. English (1984), Magma supply and storage at Kilauea volcano, Hawaii 1956–1983, *J. Volcanol. Geotherm. Res.*, *21*, 177–206.

Garcimartin, A., A. Guarino, L. Bellon, and S. Ciliberto (1997), Statistical properties of fracture precursors, *Phys. Rev. Lett.*, *79*(17), 3202–3205.

Gillard, D., M. Wyss, and J. S. Nakata (1992), A seismotectonic model for western Hawaii based on stress tensor inversion from fault plane solutions, *J. Geophys. Res.*, *97*, 6629–6641.

Gillard, D., M. Wyss, and P. Okubo (1996), Type of faulting and orientation of stress and strain as a function of space and time in Kilauea's south flank, Hawaii, *J. Geophys. Res.*, *101*, 16,025–16,042.

Grasso, J.-R., and P. Bachèlery (1995), Hierarchical organization as a diagnostic approach to volcano mechanics: Validation on Piton de la Fournaise, *Geophys. Res. Lett.*, *22*, 2897–2900.

Hanks, T. C., and H. Kanamori (1979), A moment magnitude scale, *J. Geophys. Res.*, *84*, 2348–2350.

Hill, D. P. (1977), A model for earthquakes swarms, *J. Geophys. Res.*, *82*, 1347–1352.

Johansen, A., and D. Sornette (2000), Critical ruptures, *Eur. Phys. J. b B*, *18*, 163–181.

Johnson, D. J. (1992), Dynamics of magma storage in the summit reservoir of Kilauea volcano, Hawaii, *J. Geophys. Res.*, *97*, 1807–1820.

Johnson, D. J., F. Sigmundsson, and P. T. Delaney (2000), Comment on "Volume of magma accumulation or withdrawal estimated from surface uplift or subsidence, with application to the 1960 collapse of Kilauea volcano" by P. T. Delaney and D. F. McTigue, *Bull. Volcanol.*, *61*, 491–493.

Karpin, T. L., and C. H. Thurber (1987), The relationship between earthquake swarms and magma transport: Kilauea volcano, Hawaii, *Pure Appl. Geophys.*, *125*, 971–991.

Kilburn, C. R. J., and P. R. Sammonds (2005), Maximum warning times for imminent volcanic eruptions, *Geophys. Res. Lett.*, *32*, L24313, doi:10.1029/2005GL024184.

Kilburn, C. R. J., and B. Voight (1998), Slow rock fracture as eruption precursor at Soufriere Hills volcano, Montserrat, *Geophys. Res. Lett.*, *25*, 3665–3668.

Klein, F. W., R. Y. Koyanagi, J. S. Nakata, and W. R. Tanigawa (1987), The seismicity of Kilauea's magma system, in *Volcanism in Hawaii*, *U. S. Geol. Surv. Prof. Pap.*, *1350*, 1019–1186.

Lahaie, F., and J.-R. Grasso (1998), A fluid-rock interaction cellular automaton of volcano mechanics: Application to the Piton de la Fournaise, *J. Geophys. Res.*, *103*, 9637–9649.

Lénat, J., and P. Bachèlery (1990), Structure et fonctionnement de la zone centrale du Piton de la Fournaise, in *Le Volcanisme de la Réunion*, edited by J.-F. Lénat, pp. 257–296, CRV, Clermont-Ferrand, France.

Lockwood, J. P., J. J. Dvorak, T. T. English, R. Y. Koyanagi, A. T. Okamura, M. L. Summers, and W. R. Tanigawa (1987), Mauna-Loa 1974–1984: A decade of intrusive and extrusive activity, in *Volcanism in Hawaii*, *U. S. Geol. Surv. Prof. Pap.*, *1350*, 537–570.

Lu, Z., T. Masterlark, D. Dzurisin, R. Rykhus, and C. Wicks Jr. (2003), Magma supply dynamics at Westdahl volcano, Alaska, modeled from satellite radar interferometry, *J. Geophys. Res.*, *108*(B7), 2354, doi:10.1029/2002JB002311.

Marsan, D., and G. Daniel (2007), Measuring the heterogeneity of the coseismic stress change following the 1999 M_w7.6 Chi-Chi earthquake, *J. Geophys. Res.*, *112*, B07305, doi:10.1029/2006JB004651.

McNutt, S. R. (1996), Seismic monitoring and eruption forecasting of volcanoes: A review of the state-of-the-art and case histories, in *Monitoring and Mitigation of Volcano Hazards*, edited by R. Scarpa and R. I. Tilling, pp. 99–146, Springer, New York.

Ohminato, T., B. A. Chouet, P. Dawson, and S. Kedar (1998), Waveform inversion of very long period impulsive signals associated with magmatic injection beneath Kilauea volcano, Hawaii, *J. Geophys. Res.*, *103*, 23,839–23,862, doi:10.1029/98JB01122.

Pinel, V., and C. Jaupart (2003), Magma chamber behavior beneath a volcanic edifice, *J. Geophys. Res.*, *108*(B2), 2072, doi:10.1029/2002JB001751.

Rhodes, J. M. (1988), Geochemistry of the 1984 Mauna Loa eruption: Implications for magma storage and supply, *J. Geophys. Res.*, *93*, 4453–4466.

Rubin, A. M., and D. Gillard (1998), Dike-induced earthquakes: Theoritical considerations, *J. Geophys. Res.*, *103*, 10,017–10,030.

Rubin, A. M., D. Gillard, and J.-L. Got (1998), A reinterpretation of seismicity associated with the January 1983 dike intrusion at Kilauea Volcano, Hawaii, *J. Geophys. Res.*, *103*, 10,003–10,016, doi:10.1029/97JB03513.

Sigmundsson, F., P. Durand, and D. Massonnet (1999), Opening of an eruptive fissure and seaward displacement at Piton de le Fournaise volcano measured by RADARSAT satellite radar interferometry, *Geophys. Res. Lett.*, *26*, 533–536.

Simkin, T., and L. Siebert (2000), Earth's volcanoes and eruptions: An overview, in *Encyclopedia of Volcanoes*, edited by H. Sigurdsson, pp. 249–262, Academic, San Diego, Calif.

Sturkell, E., P. Einarsson, F. Sigmundsson, S. Hreinsdttir, and H. Geirsson (2003), Deformation of Grìmsvötn volcano, Iceland: 1998 eruption and subsequent inflation, *Geophys. Res. Lett.*, *30*(4), 1182, doi:10.1029/2002GL016460.

Tilling, R. I., and J. J. Dvorak (1993), Anatomy of a basaltic volcano, *Nature*, *363*, 125–133.

Voight, B. (1988), A method for prediction of volcanic eruption, *Nature*, *332*, 125–130.

Wallace, M. H., and P. T. Delaney (1995), Deformation of Kilauea volcano during 1982 and 1983: A transition period, *J. Geophys. Res.*, *100*, 8201–8219.

Wessel, P., and W. H. F. Smith (1991), Free software helps map and display data, *Eos Trans. AGU*, *72*, 441, doi:10.1029/90EO00319.

Zapperi, S., P. Ray, H. E. Stanley, and A. Vespignani (1997), First-order transition in the breakdown of disordered media, *Phys. Rev. Lett.*, *78*(8), 1408–1411.

Zúñiga, F. R., M. Wyss, and F. Scherbaum (1988), A moment-magnitude relation for Hawaii, *Bull. Seismol. Soc. Am.*, *78*, 370–373.

V. Ferrazzini, Observatoire Volcanologique du Piton de la Fournaise, Institut de Physique du Globe de Paris, La Plaine des Cafres, La Réunion, France. (ferraz@ipgp.jussieu.fr)

J.-L. Got, O. Lengliné, D. Marsan, and V. Pinel, Laboratoire de Géophysique Interne et Tectonophysique, CNRS, Université de Savoie, Campus Scientifique, Bâtiment Belledonne, F-73376 Le Bourget du Lac Cedex, France. (jean-luc.got@univ-savoie.fr; olivier.lengline@univ-savoie.fr; david.marsan@univ-savoie.fr; virginie.pinel@univ-savoie.fr)

P. G. Okubo, U.S. Geological Survey, Hawaiian Volcano Observatory, Hawaii National Park, HI 96718, USA. (pokubo@usgs.gov)